Semiconductor Physics, Quantum Electronics & Optoelectronics, 2026. V. 29, No 2. P. 211-218.

Optics

Characterisation of detection conditions of concealed surveillance optical systems using laser-assisted cat-eye effect

L.A. Derzhypolska, Y.P. Sharlovych, A.G. Derzhypolskyi, S.V. Khodakovskyi, A.M. Negriyko

Institute of Physics, National Academy of Sciences of Ukraine, Kyiv, Ukraine
Corresponding author e-mail: d.liudmyl.flla@gmail.com

Abstract. Detection of concealed remote optical surveillance systems has become a critical issue due to ease of deployment of such systems and their ability to transmit video signals with minimal effort. This work investigates feasibility of using an active laser detection system to detect optoelectronic surveillance devices under challenging conditions, including bright daylight. The detection system is based on laser light retroreflection (the cat-eye effect), which enhances the detection efficiency due to strong back-reflection of the laser beam from optical components of the observed devices. Typical apertures of the surveillance systems such as smartphone cameras with diameters up to 2 mm and photographic lenses with diameters up to 20 mm are analyzed. Maximum detection ranges for different power levels of the active laser system are evaluated. The numerical modeling results have shown strong agreement with experimental measurements on real atmospheric paths up to 200 m. The findings confirm practical potential of active laser detection as an effective and robust method for counter-surveillance applications.

Keywords: retroreflection, smartphone cameras, photographic lenses, detection ranges, active laser detection system.

https://doi.org/10.15407/spqeo29.02.211
PACS 42.65.Jx, 42.79.Ag, 85.60.-q

Manuscript received 13.10.25; revised version received 01.05.26; accepted for publication 10.06.26; published online 23.06.26.

1. Introduction

In the context of rapid technological advancement, unauthorized use of miniature optical systems, including covert surveillance cameras, has become a growing concern for personal privacy, corporate confidentiality, and national security. These miniature devices are often difficult to detect with naked eye, making it increasingly important to develop and implement optical methods capable of revealing their presence in various environments [1–3].

Retroreflection is widely used in passive safety systems such as road signs, worker vests, and markings on vehicles. However, in recent years, this principle has been increasingly adapted to the optical detection of lenses, especially miniature camera lenses that are capable of retroreflecting directed light [4, 5]. Most often, a laser or focused LED spotlight located next to the camera or in the same optical unit with it is used for this purpose. As a result, even microscopic lenses appear as bright spots against the background of a faintly scattered image [6, 7]. The intensity of the reflected wave is, on average, 2–4 orders of magnitude higher than that from diffuse targets [8, 9]. The probability of successful lens detection can be quantitatively described by models of bidirectional retroreflection cross section and laser sight detection [10, 11].

Such technologies are of great importance for protecting private property, banking institutions, government facilities, as well as in the aviation and defense industries. For example, when inspecting hotel rooms or rented apartments, a retro-reflection-based system can detect a hidden camera in an air conditioner vent, ventilation opening, or built into furniture. In the corporate sector, this technology is used to scan for unauthorized devices in meeting or technical rooms. Mobile detection systems have already been proposed and tested for practical counter-surveillance operations [12].

In our previous works [13, 14], we investigated propagation of light in the atmosphere and interaction of laser radiation with the open atmosphere, which allowed us to simulate operation of detection systems in real conditions. This is critical for practical application for protecting private territories, buildings, perimeters, airports, or military facilities, where atmospheric effects cannot be ignored.

Analysis of the “worst-case” operating conditions of an active laser detection system, namely operation on a sunny day over open atmospheric paths, will make it possible to assess the potential for creating compact devices that can be employed in the field of protection against optical espionage. Theoretical evaluations of

critical parameters, along with real experiments, will help identify vulnerabilities of such a system and mitigate them for operation under various conditions.

2. Theoretical background of the retroreflection effect

To describe the process of detecting optoelectronic devices using retroreflection, the first stage under consideration is illumination of the scene, in which a concealed target is located (see Fig. 1).

A laser with the wavelength λ and the output power P_0 emits uniformly into a solid angle Ω_0. At a distance L, the objective lens with the aperture d_1 and the focal length f_1 forms a focused spot of the power P_1 and area S in its focal plane:

$$P_1 = \frac{P_0}{\Omega_0} \cdot \frac{\pi d_1^2}{4L^2}. \quad (1)$$

In this case, a small focal spot of the incident flux P_1 with an area S_1 is formed in the focal plane of the camera (Fig. 1). The size of this spot is defined by diffraction at the camera lens aperture and, in the absence of optical aberrations and phase distortions of the primary beam in the atmosphere, has the characteristic radius of an Airy disk and a corresponding area

$$r_1 = 1.22\frac{\lambda f_1}{d_1}, \; S_1 = \pi r_1^2 = 1.49\frac{\pi\lambda^2 f_1^2}{d_1^2} \quad (2)$$

The radiation partially reflected by the sensor matrix from the focal spot area S_1 comprises both specular and diffuse components. In the limiting case, when the specular component is absent or, due to reflection geometry, does not couple back into the objective lens, only the diffuse component contributes to the return signal. The diffuse scattering is assumed to follow a Lambertian distribution and is emitted into a solid angle of 2π. Denoting the diffuse reflection coefficient as η_1, the power of the diffusely scattered radiation recaptured by the objective lens, forming the effective retroreflection, P_2, is expressed as follows:

$$P_2 = \frac{\eta_1 P_1}{2\pi} \cdot \frac{\pi d_1^2}{4f_1^2} = \frac{\eta_1 P_0}{\Omega_0 L^2} \cdot \frac{\pi d_1^4}{32 f_1^2}. \quad (3)$$

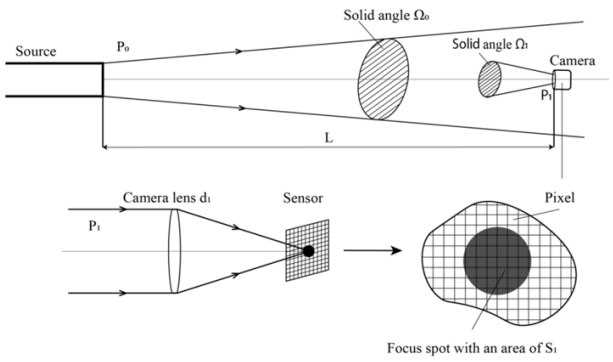

Fig. 1. Scheme of laser illuminated camera-object and the resulting focus spot S_1 on its sensor.

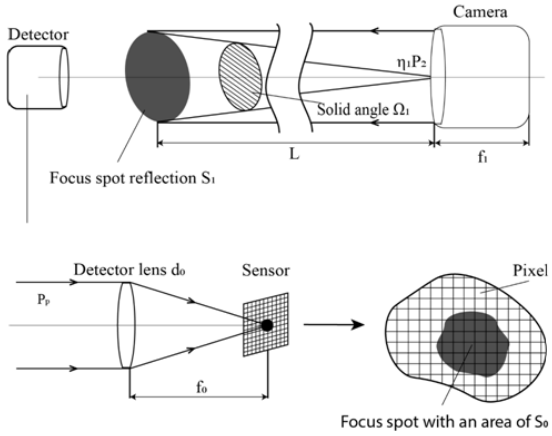

Fig. 2. Scheme of camera-detector registering reflected beam and the resulting focus spot reflection S_0.

The camera lens forms a retroreflex projection of the focal spot S_1 toward the primary source at infinity within a solid angle Ω_1.

$$\Omega_1 = \frac{S_1}{f_1^2} \approx 1.49\frac{\pi\lambda^2}{d_1^2}. \quad (4)$$

The second stage of detecting optoelectronic systems is observation. This stage is illustrated in Fig. 2.

The lens of the objective produces a retroreflective projection of the focused spot S_1 back toward the laser within a solid angle Ω_1. Considering the diffuse scattering coefficient η_1, the retroreflected power is given as P_2. For signal reception, a detector camera with the focal length f_0 and the aperture d_0 is employed. The retroreflected power P_p, defined by the solid angle, under which the object is observed, enters the aperture and is focused onto the detector array as a spot with the area S_0. In this case, it is described by the following expression:

$$P_p = \frac{P_2}{\Omega_1} \cdot \frac{\pi d_0^2}{4L^2} \approx \frac{\eta_1 P_0}{\Omega_0 L^4} \cdot \frac{\pi d_1^6 d_0^2}{\lambda^2 f_1^2}. \quad (5)$$

Retroreflection detection is the most difficult in sunlight due to strong background light from scattered solar radiation, as illustrated in Fig. 3, which shows the 'worst-case scenario' for optoelectronic systems under conditions of significant solar background illumination.

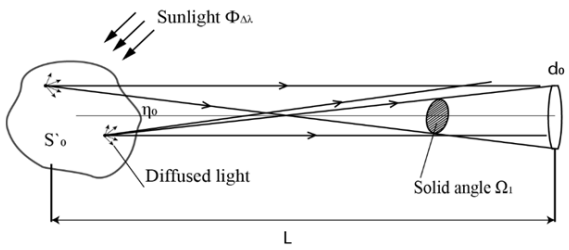

Fig. 3. The effect of sunlight on retroreflection detection.

The projection of the focal spot S_0 (the spot where the beam is focused on the detector matrix, defined similarly to S_1) onto the observation plane at a distance L will have an area S_0' which is expressed as follows:

$$S_0' = S_0 \frac{L^2}{f_0^2} = 1.49 \frac{\pi \lambda^2 L^2}{d_0^2}. \quad (6)$$

Solar flux with the spectral irradiance $\Phi_{\Delta\lambda}$ illuminates the observation plane within the detector spectral range $\Delta\lambda$. The solar power on the area S_0' is $P_0' = \Phi_{\Delta\lambda} \cdot S_0'$. The surfaces within S_0' have the scattering coefficient η_0 and Lambertian behavior. The power of the scattered background light entering the aperture d_0 and focused on the spot S_0 is P_p' described by the following expression:

$$P_p' = \frac{\eta_0 P_0'}{2\pi} \cdot \frac{\pi d_0^2}{4L^2} \approx \pi \eta_0 \lambda^2 \Phi_{\Delta\lambda}. \quad (7)$$

As a criterion for reliable detection, we assume that the power of the retroreflex signal must be at least ten times greater than the background signal observed in daylight conditions: $P_p / P_p' \geq 10$. Using this criterion, the minimum source power $P_{0\min}$ required for detecting at the maximum specified distance $L_{\max}$ can be calculated as follows:

$$P_{0\min} \sim \Omega_0 \lambda^4 L^4 f_1^2 \Phi_{\Delta\lambda} d_1^{-6} d_0^{-2}, \quad (8)$$

$$L_{\max} \sim \sqrt[4]{\frac{\eta_1 P_0 d_1^6 d_0^2}{\eta_0 \Omega_0 \lambda^4 f_1^2 \Phi_{\Delta\lambda}}}. \quad (9)$$

3. Theoretical analysis of the retroreflection effect

For analyzing results of theoretical calculations and experiments, we used two standard types of cameras-objects:

- ✓ "small camera": f_1 = 5 mm, d_1 = 2 mm (standard size of cameras used for covert surveillance or a mobile phone camera);
- ✓ "large camera": f_1 = 50 mm, d_1 = 20 mm (standard size of cameras used in everyday photography and video recording).

In all calculations, the following detector parameters were used: $\lambda \approx 1000$ nm, $d_0 = 5$ mm, and $\Phi_{\Delta\lambda} = 7 \text{W/m}^2$. (Solar radiation flux within a spectral bandwidth of 10 nm at a wavelength of 1 μm was considered. This assumption corresponds to validation of the theoretical results through an experiment conducted using a narrowband filter with a transmission bandwidth of 10 nm and a central wavelength of 980 nm.) Each solid angle value for the calculations was chosen to cover the entire range from $\Omega = 10^{-6}$ sr, which stands for almost perfectly collimated laser beam, to $\Omega = 1.22 \cdot 10^{-1}$ sr, which represents wide angle diode. To ensure that our range-and-power estimates remain valid under realistic daylight conditions, all background-noise and detection-threshold calculations have been performed using the ASTM G173-03 reference spectrum for terrestrial sunlight [15].

3.1. Maximum range $L_{\max}$ *vs* target aperture d_1

For both power levels, we hold the beam solid angle Ω fixed at six representative values and sweep the target aperture from 0.5 to 10 mm.

At P_0 = 10 W (Fig. 4), the curves exhibit a super-linear growth, closely following the theoretical scaling $L_{\max} \propto d_1^{1.5}$. Narrow-angle beams ($\Omega \leq 10^{-4}$ sr) already reach several hundred meters when d_1 exceeds a few millimeters, while wide beams ($\Omega \approx 0.1$ sr) remain below 100 m even at the largest apertures.

At P_0 = 100 W (Fig. 5), the same $d_1^{1.5}$ trend is preserved, but all the curves shift upward by the factor ≈ 1.78. Now, millimeter-scale apertures can push narrow beams up to and beyond 1 km, demonstrating dramatic benefit of higher power in conjunction with modest aperture increases.

These results demonstrate that doubling the target diameter yields a roughly $2^{1.5} \approx 2.82$-fold increase in the range. Meanwhile, increasing P_0 by a factor of 10 raises $L_{\max}$ by about 78%.

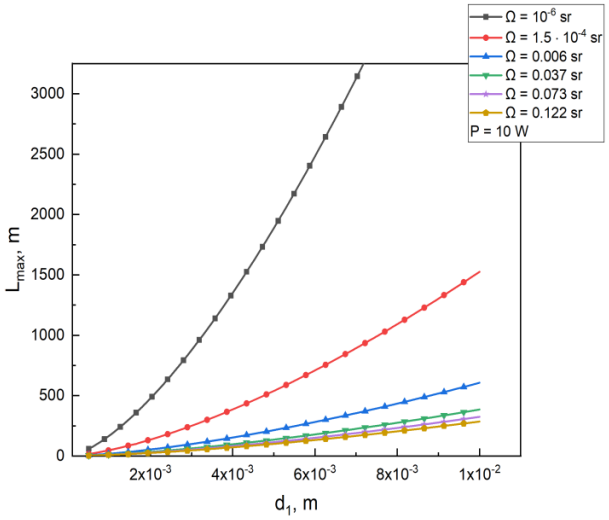

Fig. 4. $L_{\max} = f(d_1)$ at P = 10 W under different laser beam focusing conditions.

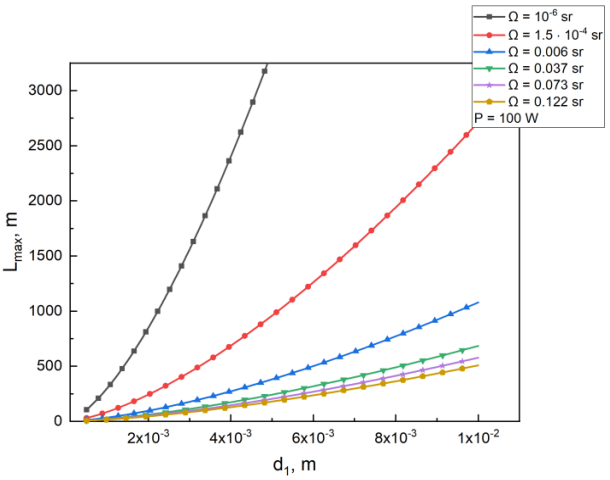

Fig. 5. $L_{\max} = f(d_1)$ at P = 100 W under different laser beam focusing conditions.

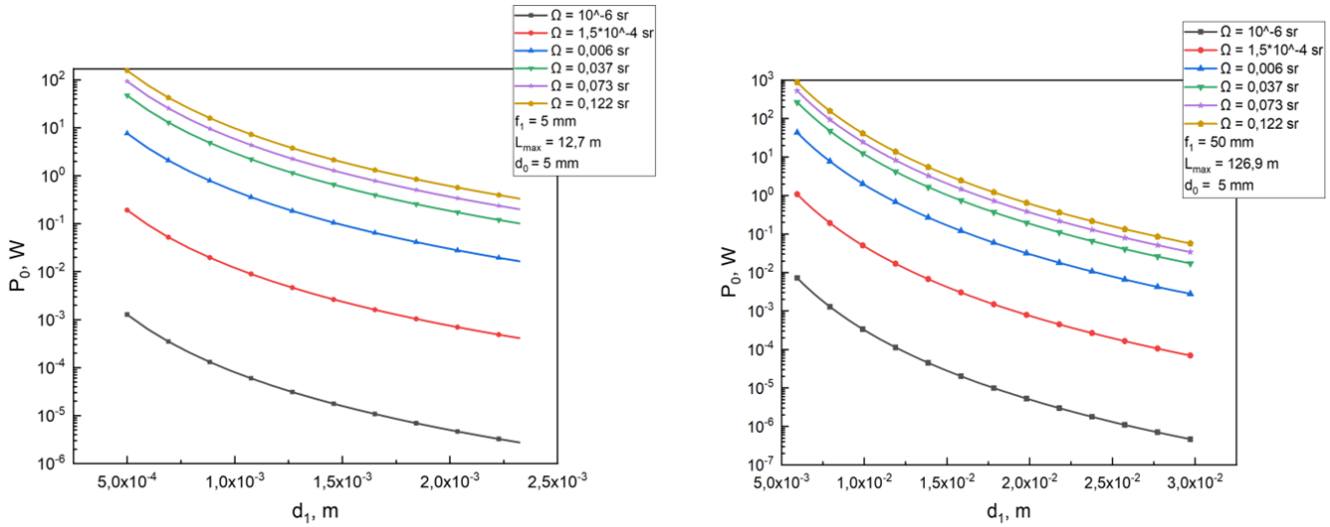

Fig. 6. $P_0 = f(d_1)$ at fixed L_{max} under different laser beam focusing conditions for small and large camera (from left to right).

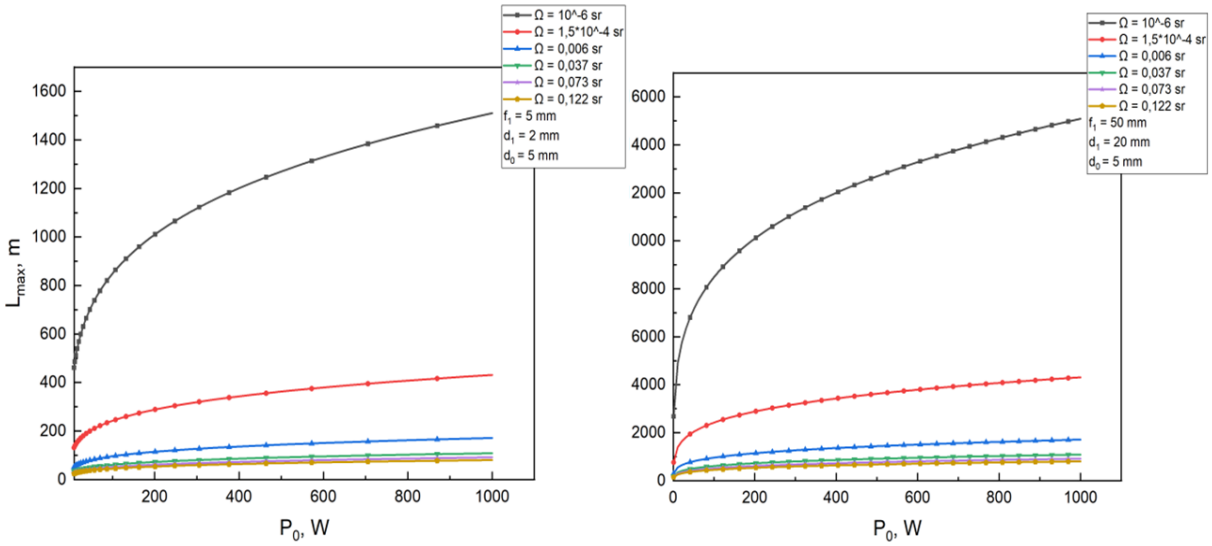

Fig. 7. $L_{max} = f(P_0)$ at fixed d_1 under different laser beam focusing conditions for small and large camera (from left to right).

3.2. Required source power P_0 *vs* target aperture d_1 for "small" *vs* "large" camera configurations

We invert the relationship presented above for a fixed detection range L_{max} = 12.7 m for small cameras and L_{max} = 126.9 m for large cameras to determine the required optical power that the laser must deliver as d_1 varies.

In the "small camera" case (Fig. 6), $P_0 \propto d_1^{-4}$. Increase in the aperture diameter from 0.5 to 2.5 mm reduces the required power by more than two orders of magnitude. However, for wide-angle beams ($\Omega \approx 0.1$ sr), even a 2.5 mm aperture demands hundreds of watts to reach the target range L_{max}.

In the "large camera" case, the same d_1^{-4} decline is observed but with a far lower baseline. Now, a few watts suffice for solid angles of the order of $\Omega \approx 10^{-2}$ sr (the aperture diameter varies from 5 to 30 mm), and even wide beams become feasible at tens of watts.

Increasing the receiver aperture size is by far the most effective way to reduce laser power requirements, especially in constrained "small camera" systems. Yet, "large camera" architectures offer an additional orders-of-magnitude improvement.

3.3. Range L_{max} *vs* required source power P_0 for "small" *vs* "large" camera configurations

Finally, we plot P_0 *versus* L_{max} for both camera classes at all six values of Ω. Both sets of curves (Fig. 7) confirm the $P_0 \propto L_{max}^4$ law.

In the "small camera" case, to double the range from 100 to 200 m would require a 16-fold increase in P_0, quickly reaching impractical hundreds of watts for wider beams. In the "large camera" case, the same doubling increases the power by the same factor of 16. However, because of the much lower baseline power, even

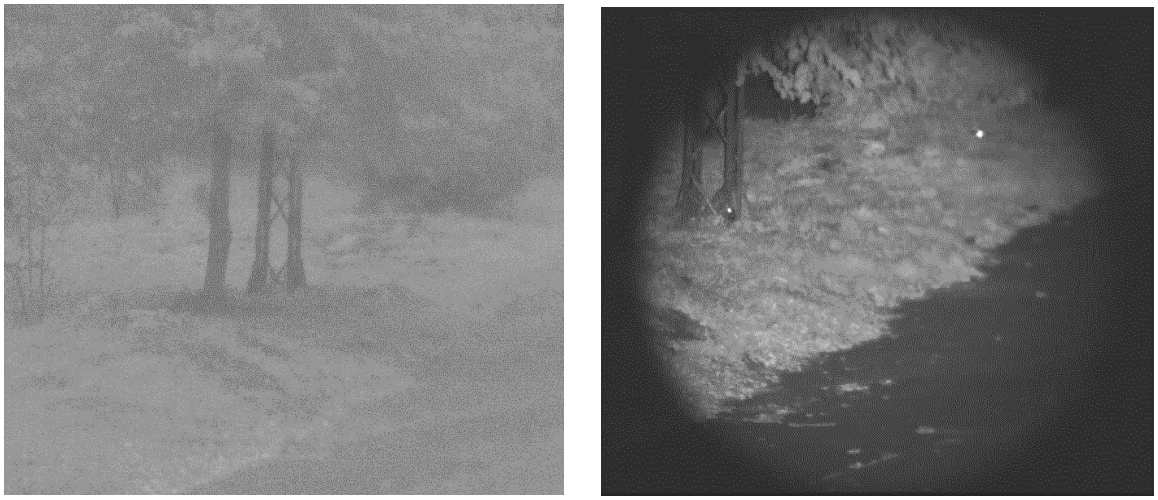

Fig. 8. Detection of a "small camera" at $L \approx 100$ m, $P = 10$ W, $\Omega_0 \approx 1 \cdot 10^{-4}$ sr, and $\lambda = 980$ nm.

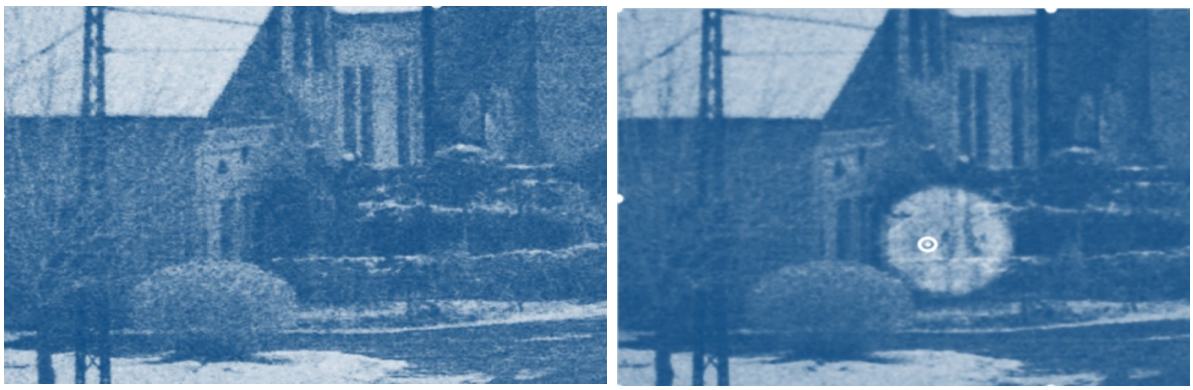

Fig. 9. Area with a hidden "large camera" at $L \approx 100$ m. Detection of the "large camera" at $P = 1.5$ W, $\Omega_0 \approx 2 \cdot 10^{-2}$ sr, and $\lambda = 980$ nm.

kilometer-scale detection for moderate divergences ($\Omega \approx 10^{-3}$ sr) requires under tens of watts. The fourth-power dependence of the power on range imposes severe constraints on long-distance operation. Pairing modest beam divergences with larger optics is essential to tame power growth into a practical regime.

4. Experimental verification of the retroreflection effect

To validate the active detection system, experimental tests under real atmospheric conditions at a distance $L \approx 100$ m during daylight were conducted. A complementary metal-oxide-semicondutor (CMOS) camera equipped with a narrowband filter (10 nm bandwidth) tuned to the laser wavelength $\lambda = 980$ nm was used to detect two types of targets:

- ✓ In the "small camera" case ($f_1 = 5$ mm, $d_1 = 2$ mm, $\Omega_0 = 1 \cdot 10^{-4}$ sr), the laser operated at a power $P_0 = 10$ W (Fig. 8).
- ✓ In the "large camera" case ($f_1 = 50$ mm, $d_1 = 20$ mm, $\Omega_0 = 2 \cdot 10^{-2}$ sr), the laser operated at a power $P_0 = 1.5$ W (Fig. 9).

In all the conducted experiments, the retroreflected signal remained above the detection threshold.

On the left side of Fig. 8, using a camera-detector, we observe the scene with concealed optoelectronic sensors – passive detection. The target cameras are not detected under passive observation. On the right side, we have active detection – the laser is turned on. The large bright spot corresponds to the diameter of the laser beam, and two the brightest points correspond to the two concealed optoelectronic sensors.

In Fig. 9, similar to Fig. 8, the left side shows the scene under passive detection. On the right side, we observe the concealed target thanks to active detection (the brightest point is circled).

Therefore, the small-camera experiment used roughly a 5-fold power margin, and the large-camera experiment used a 40-fold margin relative to the idealized minimum. The following safety factors are expected: real-world losses – imperfect optical throughput at 980 nm, detector quantum efficiency, pointing jitter, atmospheric absorption and scattering, and background noise.

Despite these non-modeled inefficiencies, both measured points lie well above the theoretical curves and confirm quartic range scaling. For future system design, reducing the required P_0 will demand improved end-to-end efficiency at the operating wavelength, tighter beam divergence and/or larger effective apertures. In practical terms, these results validate our model and quantify the margins necessary to achieve reliable detection at 100 m in real-world conditions.

5. Discussion

The results obtained in this work demonstrate that the proposed active laser-based retroreflection detection method remains efficient under daylight conditions and can reliably identify optoelectronic systems with apertures ranging from 2 to 20 mm. The theoretical predictions, including the $L_{\max} \propto d_1^{1.5}$ and $P_0 \propto L_{\max}^4$ scaling laws, are validated experimentally at a 100 m atmospheric path. Nevertheless, several practical considerations must be addressed to assess full applicability of the approach in real environments.

5.1. Comparison to other detection methods

Recent literature reports several alternative techniques for concealed-camera detection. Smartphone-based systems use the built-in flash or time-of-flight sensors to induce retroreflection from nearby lenses, offering portability. However, they are limited to the ranges of a few meters and strongly depend on the camera rolling-shutter timing and ambient light [3]. Image-sensor-based approaches employing CMOS/ToF arrays or avalanche-photodiode scanning systems [6] can detect lenses with high spatial resolution, yet they typically require complex scanning or high-sensitivity detectors to overcome background illumination.

Compared to these methods, the laser-based approach studied here ensures significantly larger detection distances (tens to hundreds of meters) and is less sensitive to focusing errors, because the cat-eye return is governed primarily by the target aperture and divergence of the incident beam. The method also scales predictably with power and optics size, enabling quantitative design of field-deployable systems.

5.2. Influence of atmospheric turbulence

Although the experimental results validate the model under relatively stable conditions, atmospheric turbulence introduces additional fluctuations to the received signal. Turbulence leads to beam wander, beam spreading and scintillation, all of them reducing the average irradiance on the target and modifying the return flux. Accounting for turbulence may therefore require implementing adaptive beam-pointing stabilization or using partially coherent beams to mitigate intensity fluctuations.

5.3. Detector noise and system limitations

In practical scenarios, the sensitivity of the detection camera sets an additional constraint. Shot noise, dark current, readout noise, and limited quantum efficiency at the laser wavelength reduce the effective signal-to-noise ratio. The experiments presented here intentionally operated with a power margin (5-fold for the small-aperture and 40-fold for the large-aperture configuration) to overcome losses due to detector inefficiency and optical throughput. In optimized systems, use of higher-sensitivity detectors, improved filters, or cooled sensors could reduce the required laser power, especially for long-range applications.

Overall, while the laser retroreflection method demonstrates clear advantages in range and robustness, its practical performance depends on careful balancing of beam divergence, power, atmospheric effects, and detector characteristics. These aspects should be considered during designing compact operational systems for counter-surveillance applications.

6. Conclusions

This study analyzes the key parameters that affect the guaranteed detection of optical systems using the retroreflex method under daylight conditions.

The analysis focuses on four main factors: laser output power, beam divergence, aperture diameter of the concealed camera optical system (target), and detection range. The minimum required power of the laser detection system and the maximum achievable detection distance were determined taking into account influence of daylight background illumination, which significantly reduces the guaranteed detection threshold.

It was theoretically shown and experimentally confirmed that the minimum required source power and the maximum detection range are related by a fourth-power dependence. That is, each doubling of the detection distance requires a sixteen-fold increase in the laser power. It was established as well that the aperture diameter of the target optical system appears in the sixth power in the denominator of the general equation, which explains why even a slight increase in the target lens aperture can substantially reduce the required laser power.

Since the minimum power required for detecting a concealed target is directly proportional to the beam divergence, a logical recommendation is to minimize divergence when using low-power laser systems. However, this approach requires implementation of a scanning system and precise beam-pointing control. Quantitative estimates of the active laser detection system's performance were made using the ASTM G173-03 reference daylight spectrum to ensure the reliability of the results under real-world illumination conditions.

Acknowledgements

This research was supported by the National Research Foundation of Ukraine through the project No. 228/0148 "Research and development of advanced methods and technologies for the generation and formation of high-energy laser beams for defense applications and post-war environmental restoration".

References

1. Solanki R.S., Khurana V. Studies on retro-reflection for optical target detection. *J. Opt.* 2024. **53**. P. 336–341. https://doi.org/10.1007/s12596-023-01308-5.
2. Seets T., Epstein A., Velten A. Watching the watchers: camera identification and characterization using retro-reflections. *Opt. Exp.* 2024. **32**. P. 13836–13850. https://doi.org/10.1364/OE.520545.
3. Sami S., Tan S.R.X., Sun B., Han J. LAPD: Hidden spy camera detection using smartphone time-of-flight sensors, *SenSys'21: Proc. 19th ACM Conf. on Embedded Networked Sensor Systems.* P. 288–301. https://doi.org/10.1145/3485730.3485941.
4. Auclair M., Sheng Y., Fortin J. Identification of targeting optical systems by multiwavelength retroreflection. *Opt. Eng.* 2013. **52**, No 5. P. 054301. https://doi.org/10.1117/1.OE.52.5.054301.
5. Mieremet A.L., Schleijpen R.M.A., Pouchelle P.N. Modeling the detection of optical sights using retro-reflection. *Proc. SPIE*. 2008. **6950**. P. 69500E-1. https://doi.org/10.1117/12.774634.
6. Svedbrand D., Allard L., Pettersson M. *et al.* Optics detection using an avalanche photo diode array and the scanning-slit-method. *Proc. SPIE*. *Technologies for Optical Countermeasures XVI*. 2019. **11161**. P. 111610J. https://doi.org/10.1117/12.2531795.
7. Gong M., He S., Guo R., Wang W. Cat-eye effect reflected beam profiles of an optical system with sensor array. *Appl. Opt.* 2016. **55**. P. 4461–4466. https://doi.org/10.1364/AO.55.004461.
8. Liang G.C., Wei H.Z., Song J.Y. *et al.* Target classification with 'cat eye effect'. *High Power Laser Particle Beams*. 2003. **15**, No 7. P. 632–634.
9. Zhao Y., Sun H., Yu X., Fan M. Three-dimensional analytical formula for oblique and off-axis Gaussian beams propagating through a cat-eye optical lens. *Chin. Phys. Lett.* 2010. **27**, No 3. 034101. https://doi.org/10.1088/0256-307X/27/3/034101.
10. Lecocq C., Deshors G., Lado-Bordowsky O., Meyzonnette J.L. Sight laser detection modeling. *Proc. SPIE*, *Laser Radar Technology and Applications VIII.* 2003. **5086**. https://doi.org/10.1117/12.486055.
11. Laurenzis M., Christnacher F., Matwyschuk A. *et al.* Electro-optical detection probability of optical devices determined by bidirectional laser retro-reflection cross section. *Proc. SPIE*, *Radar Sensor Technology XIX; and Active and Passive Signatures VI*. 2015. **9461**. P. 94611L. https://doi.org/10.1117/12.2175858.
12. Sadler L., Alexander A. Mobile optical detection system for counter surveillance. *Proc. SPIE, Ground/ Air Multi-Sensor Interoperability, Integration, and Networking for Persistent ISR.* 2010. **7964**. P. 76940Y. https://doi.org/10.1117/12.850465.
13. Matsniev I., Andriichuk V., Chumak O. *et al.* The threshold of laser-induced damage of image sensors in open atmosphere. *Nanoelectronics, Nanooptics, Nanochemistry and Nanobiotechnology, and Their Applications . NANO 2022. Springer Proceedings in Physics.* 2023. **297**. 299–322. https://doi.org/10.1007/978-3-031-42708-4_20.
14. Andriichuk V., Derzhypolska L., Matsniev I., Chumak O. Analysis of beam wandering and influence of partial coherence on fourth-order moment of the light field in turbulent atmosphere. *Optik.* 2025. **321**. P. 172156. https://doi.org/10.1016/j.ijleo.2024.172156.
15. https://pvlib-python.readthedocs.io/en/latest/gallery/spectrum/plot_standard_ASTM_G173-03.html.

Authors and CV

Liudmyla Derzhypolska, PhD in Physics and Mathematics, Senior Research Scientist at the Department of Laser Spectroscopy, Institute of Physics NASU. Author of 20 publications. Her research focuses on laser beam propagation in the atmosphere, formation of focused energy spots on distant targets, development of compact high-efficiency laser sources (Nd:YAG, Yb:YAG), and methods of long-range detection of optical elements. https://orcid.org/0000-0001-6412-7797

Yaroslav Sharlovych, Currently pursuing a Master's degree in Optics and Laser Physics at the Taras Shevchenko National University of Kyiv. Associate Researcher at the Institute of Physics NASU (2024 – presently). His scientific interests include experimental optics, laser physics, and optical detection systems.

Andrii Derzhypolskyi, PhD in Physics and Mathematics, Research Scientist at the Department of Laser Spectroscopy, Institute of Physics NASU. Author of 22 publications. His research focuses on Fourier holography systems with identical reference and object beams, mathematical modeling of virtual optical systems, and development of advanced methods for information storage, transmission, and encryption resistant to interference and distortions. https://orcid.org/0000-0003-3805-5317

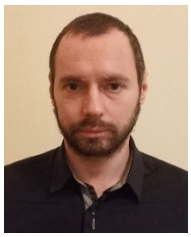

Serhii Khodakovskyy, Bachelor of Mathematics, Associate Researcher at the Institute of Physics NASU. His research focuses on software development for laser spectrometry and laser-induced breakdown spectroscopy (LIBS) experiments. https://orcid.org/0000-0002-9187-5093

Anatoliy Negriyko, Doctor of Sciences in Physics and Mathematics, Head of the Laser Spectroscopy Research Department, Institute of Physics NASU and Associate Professor at the NTUU "Igor Sikorsky Kyiv Polytechnic Institute". Author of 114 publications. His research focuses on laser-matter interactions with atoms, molecules, and micro- and nanoparticles, and laser metrology and instrumentation. https://orcid.org/0000-0002-2954-5157

Authors' contributions

Derzhypolska L.A.: key ideas, conceptualization, investigation, formal analysis, supervision, writing – original draft.
Sharlovych Y.P: investigation, formal analysis.
Derzhypolskyi A.G.: key ideas, conceptualization, investigation, writing – review & editing.
Khodakovskyi S.V.: validation, resources, investigation.
Negriyko A.M.: key ideas, formal analysis, supervision.

Характеризація умов детектування прихованих оптичних систем спостереження за ефектом «котячого ока» з лазерною підсвіткою

Л.А. Держипольська, Я.П. Шарлович, А.Г. Держипольський, С.В. Ходаковський, А.М. Негрійко

Анотація. Виявлення прихованих віддалених оптико-електронних систем спостереження стало важливим завданням через простоту їх розгортання та здатність передавати відеосигнали з мінімальними зусиллями. У даній роботі досліджено можливість використання активної лазерної системи для виявлення оптико-електронних пристроїв спостереження в складних умовах, зокрема за яскравого денного освітлення. Основою лазерної системи є ефект ретрорефлексу, відомий як ефект «котячого ока», який підвищує ефективність виявлення завдяки сильному зворотному відбиттю лазерного пучка від оптичних елементів спостережуваних пристроїв. Проаналізовано типові апертури систем спостереження, такі як камери смартфонів із діаметром до 2 мм та фотографічні об'єктиви з діаметром до 20 мм. Оцінено максимальні дальності виявлення для різних рівнів потужності активної лазерної системи. Результати числового моделювання показали високу відповідність експериментальним вимірюванням, виконаним на реальних атмосферних трасах до 200 м. Отримані результати підтверджують практичний потенціал активного лазерного виявлення як ефективного та надійного методу для контрспостережних застосувань.

Ключові слова: ретрорефлекс, камери смартфонів, фотографічні лінзи, дальності виявлення, активна лазерна система виявлення.